Line-by-line pulse shaping with spectral resolution below 890 MHz

John T. Willits,[1,2] Andrew M. Weiner,[1,3,4] and Steven T. Cundiff[1,2,*]

[1] *JILA, University of Colorado and National Institute of Standards and Technology, Boulder Colorado 80309-0440 USA*

[2]*Department of Electrical and Computer Engineering, University of Colorado, Boulder, Colorado 80309-0425 USA*

[3]*Department of Electrical and Computer Engineering, Purdue University, West Lafayette, Indiana 47907-2035 USA*

[4]*Purdue is Andrew Weiner's current and permanent location*

[*]*cundiff@jila.colorado.edu*

Abstract: Line-by-line pulse shaping is demonstrated on a 890 MHz repetition rate mode-locked titanium sapphire laser. The high resolution pulse shaper is based on a virtual imaged phased array (VIPA) with a free spectral range of 25 GHz. For our implementation, the mask repeats every VIPA free spectral range, which corresponds to every 28 comb lines. Individual frequency modes from the laser are also resolved using the same VIPA paired with a diffraction grating to achieve a resolution of 357 MHz. Several output waveforms are compared with simulation to understand differences with the ideal case.

OCIS codes: (320.0320) Ultrafast optics; (320.5540) Pulse shaping.

References and links

1. A. M. Weiner, "Femtosecond pulse shaping using spatial light modulators," Rev. Sci. Instrum. **71**(5), 1929–1960 (2000).
2. D. J. Jones, S. A. Diddams, J. K. Ranka, A. Stentz, R. S. Windeler, J. L. Hall, and S. T. Cundiff, "Carrier-envelope phase control of femtosecond mode-locked lasers and direct optical frequency synthesis," Science **288**(5466), 635–639 (2000).
3. J. Ye and S. T. Cundiff, *Femtosecond Optical Frequency Comb Technology* (Springer, 2005).
4. Z. Jiang, D.-S. Seo, D. E. Leaird, and A. M. Weiner, "Spectral line-by-line pulse shaping," Opt. Lett. **30**(12), 1557–1559 (2005).
5. S. T. Cundiff and A. M. Weiner, "Optical arbitrary waveform generation," Nat. Photonics **4**(11), 760–766 (2010).
6. J. T. Willits, A. M. Weiner, and S. T. Cundiff, "Theory of rapid-update line-by-line pulse shaping," Opt. Express **16**(1), 315–327 (2008).
7. R. P. Scott, N. K. Fontaine, J. P. Heritage, and S. J. B. Yoo, "Dynamic optical arbitrary waveform generation and measurement," Opt. Express **18**(18), 18655–18670 (2010).
8. R.P. Scott, N. K Fontaine, D.J. Geisler, T. He, J.P. Heritage, and S.J.B. Yoo, "Demonstration of dynamic optical arbitrary waveform generation with 5-ns record lengths and 33-ps features," CLEO 2011, paper CWH5 (2011).
9. S. A. Diddams, L. Hollberg, and V. Mbele, "Molecular fingerprinting with the resolved modes of a femtosecond laser frequency comb," Nature **445**(7128), 627–630 (2007).
10. A. Bartels, T. Dekorsy, and H. Kurz, "Femtosecond Ti:sapphire ring laser with a 2-GHz repetition rate and its application in time-resolved spectroscopy," Opt. Lett. **24**(14), 996–998 (1999).
11. Z. Jiang, C. B. Huang, D. E. Leaird, and A. M. Weiner, "Optical arbitrary waveform processing of more than 100 spectral comb lines," Nat. Photonics **1**(8), 463–467 (2007).
12. M. Shirasaki, "Large angular dispersion by a virtually imaged phased array and its application to a wavelength demultiplexer," Opt. Lett. **21**(5), 366–368 (1996).
13. S. Xiao, A. M. Weiner, and C. Lin, "Experimental and theoretical study of hyperfine WDM demulitplexer performance ssing the virtually imaged phased-array (VIPA)," J. Lightwave Technol. **23**(3), 1456–1467 (2005).
14. T. K. Chan, J. Karp, R. Jiang, N. Alic, S. Radic, C. F. Marki, and J. E. Ford, "1092 channel 2-D array demultiplexer for ultralarge data bandwidth," J. Lightwave Technol. **25**(3), 719–725 (2007).
15. S. Xiao and A. Weiner, "2-D wavelength demultiplexer with potential for >/= 1000 channels in the C-band," Opt. Express **12**(13), 2895–2902 (2004).
16. S. Xiao and A. M. Weiner, "An eight-channel hyperfine wavelength demultiplexer using a virtually imaged phased-array (VIPA)," IEEE Photon. Technol. Lett. **17**(2), 372–374 (2005).
17. G. H. Lee and A. M. Weiner, "Programmable optical pulse burst manipulation using a virtually imaged phased array (VIPA) based Fourier transform pulse shaper," J. Lightwave Technol. **23**(11), 3916–3923 (2005).

#159985 - $15.00 USD Received 14 Dec 2011; revised 18 Jan 2012; accepted 20 Jan 2012; published 25 Jan 2012

18. V. R. Supradeepa, E. Hamidi, D. E. Leaird, and A. M. Weiner, "New aspects of temporal dispersion in high resolution Fourier pulse shaping: A quantitative description with virtually imaged phased array pulse shapers," J. Opt. Soc. Am. B **27**(9), 1833–1844 (2010).
19. S. J. Xiao, A. M. Weiner, and C. Lin, "A dispersion law for virtually imaged phased-array spectral dispersers based on paraxial wave theory," IEEE J. Quantum Electron. **40**(4), 420–426 (2004).

1. Introduction

Optical pulse shaping is useful for a variety of fields including high field physics, coherent control of chemical processes, and ultrafast spectroscopy [1]. The shape of optical pulses can be controlled by spectral decomposition where the phase and amplitude of the spectral components of a laser pulse are modified to produce the desired output pulse shape. Typically the output pulses can be treated as isolated pulses because the output duration is much shorter than the time between pulses. If this is not the case, then the effect of the pulse shaper must be discussed in terms of the spectrum of a pulse train, not an isolated pulse. The spectrum of a pulse train consists of discrete spectral components separated by the repetition rate of the optical pulse train, referred to as a frequency comb. Creating output waveforms that can fill the time between input pulses requires the ability to control individual components of the frequency comb. This situation is referred to as line-by-line pulse shaping because it means that the resolution elements of the pulse shaper correspond to individual lines of the comb spectrum of the pulse train. Using femtosecond comb techniques [2,3], the comb can be made sufficiently stable to make line-by-line pulse shaping possible. Line-by-line pulse shaping requires a spectral disperser with enough resolution to resolve, and a spectral mask that can manipulate, the discrete spectral components that comprise the original broadband pulse train [4]. These modified spectral components are then recombined to form the output pulse train, resulting in a repetitive output waveform that is limited only by the input bandwidth.

Line-by-line pulse shaping is an important step toward optical arbitrary waveform generation (OAWG) [5–7], where the spectral mask is updated at the repetition rate of the input laser in addition to resolving individual comb lines (note that some authors use "static OAWG" to designate line-by-line shaping and "dynamic OAWG" to designate the more difficult goal of updating the mask for every input pulse). Substantial progress has been made towards OAWG [8], although it has not been demonstrated due to the difficulty of simultaneously achieving high spectral resolution and high modulation rate.

Current line-by-line pulse shapers work for input pulse trains with high repetition rates around 10 GHz. Decreasing the repetition rate of the input pulse train requires an increase in the spectral resolution to resolve the individual comb lines. Previous high resolution setups resolved the individual modes from a 3 GHz pulse train [9]. Our static line-by-line pulse shaping setup resolves the individual modes from an 890 MHz repetition rate mode-locked titanium sapphire laser [10], modifies them and recombines them into a pulse-shaped output. This line-by-line pulse shaper with 357 MHz resolution, corresponding to a resolving power of ~10^6, periodically maps a static mask pattern onto the optical spectrum. The spectral resolution demonstrated here is, to the best of our knowledge, the highest reported in pulse shaping, an important step toward OAWG. For line-by-line shaping, the lowest comb spacing previously reported was five GHz using a grating-based shaper and generating the comb using electro-optic modulation [11]. Thus our results represent a reduction by more than a factor 5 in comb spacing for line-by-line pulse shaping. Reaching the 1 GHz level is an important milestone as it allows the combs produced by 1 GHz repetition rate modelocked Ti:sapphire lasers to be shaped without using a filter cavity.

2. Setup

The high spectral resolution setup shown in Fig. 1(a) uses two spectrally dispersive elements to resolve the individual lines of an 890 MHz frequency comb. The input pulse train is focused by a 25 cm focal length cylindrical lens into the window of a virtually imaged phased array (VIPA) [12,13]. The solid fused silica VIPA is 10 mm wide by 10 mm high with a thickness of 4.1 mm. It was designed to have a free spectral range (FSR) of 25 GHz; the measured FSR is 24.932 GHz at 808 nm. The reflectivity of the output surface was designed

#159985 - $15.00 USD Received 14 Dec 2011; revised 18 Jan 2012; accepted 20 Jan 2012; published 25 Jan 2012

to be 98.5% while the input side is over 99% reflective, which would give a theoretical resolution of 250 MHz. This value is smaller than the measured resolution of 357 MHz. The difference is attributed to manufacturing imperfections in the flatness and parallelism of the surfaces. The transition between the high reflector and window on the input surface is less than 100 μm and the input angle of the VIPA is set to 1.01°. While a VIPA provides very high spectral resolution, it overlaps comb lines separated by integer multiples of the FSR; if individual comb lines are to be resolved, another dispersive element is necessary. A grating is used to separate the repeated modes of the VIPA, where the dispersive directions of the grating and VIPA are orthogonal. The grating must have a resolution better than 25 GHz = 0.05 nm at 800 nm in the horizontal direction (x) to resolve the repeated modes of the VIPA. To achieve this resolution for a grating with 1200 lines/mm, at least 12 mm of the grating must be illuminated. This requirement is met by inserting a horizontal beam-expanding telescope before the grating. It is important to avoid expanding the beam in the vertical direction (y) after the VIPA as expansion before the spherical imaging lens interferes with proper separation of comb lines in y. For this reason, cylindrical lenses, separated by the sum of their focal lengths (10+100=110 cm), are used to expand the beam by a factor of 10 in the horizontal direction only. Finally, the light from the grating is imaged with a 50 cm focal length spherical lens onto a charge coupled device (CCD) camera. Figure 2 is an image of these individually resolved frequencies. Using the fine resolution of the VIPA to separate adjacent comb lines in y and the coarse resolution of the grating to separate repeated modes of the VIPA in x, a two-dimensional frequency 'brush' is created [9,14,15].

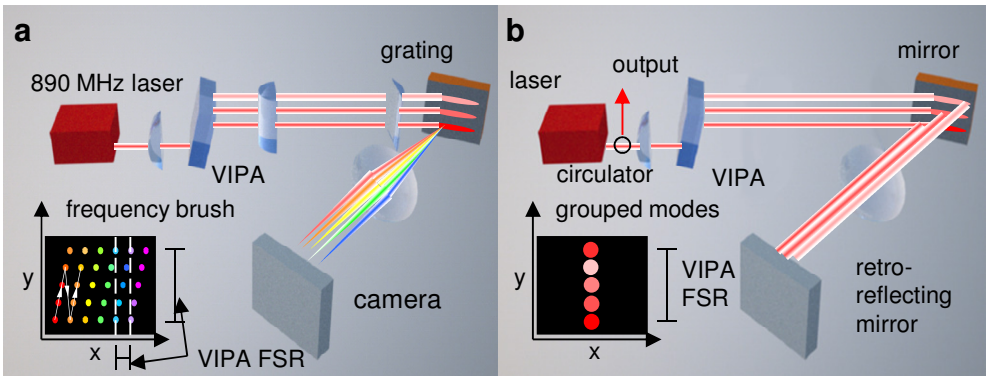

Fig. 1. The high resolution setup (a) resolves individual comb lines spaced by 890 MHz. The VIPA with a FSR of 25 GHz separates adjacent comb lines in the y direction and the grating separates repeated orders of the VIPA along the x direction. The white arrows show adjacent comb lines with increasing frequency. The 1-D VIPA only based pulse shaper (b) shows how by removing the grating and horizontal beam expander adjacent frequency modes are resolved into separate groups. These groups of comb lines can then be modified to perform line-by-line pulse shaping with spectral masks that repeat every VIPA FSR.

A tunable continuous wave (CW) laser is used to calibrate the frequency sensitivity, measure the resolution and analyze the crosstalk between frequency modes of the brush image. First, the frequency sensitivity of the brush image can be calculated by measuring the number of pixels between two known frequencies. Figure 3(a) shows the images of two CW frequencies separated by 25 pixels with 890 MHz difference between them, which corresponds to a frequency sensitivity of 28.0 pixels/GHz. This calculation can be repeated at different frequencies to test the frequency sensitivity over the entire VIPA FSR. Due to the nonlinear spectral dispersion characteristic of the VIPA (see below), the frequency sensitivity varies over the FSR from 26.9 to 35.9 pixels/GHz with an average sensitivity of 30.9 pixels / GHz. The larger values only occur at the edge of the image and thus only for 6 comb lines is the variation above 32.5 pixels/GHz. Next, the spectral resolution can be measured from the full width half maximum (FWHM) of the lineshape. The FWHM in Fig. 3(a) is 10 pixels, which corresponds to a resolution of 357 MHz. Finally, by comparing two frequencies

#159985 - $15.00 USD Received 14 Dec 2011; revised 18 Jan 2012; accepted 20 Jan 2012; published 25 Jan 2012

separated by the comb spacing, 890 MHz, the crosstalk between adjacent comb lines can be estimated. As seen in Fig. 3(a), each line has a tail toward higher frequency (for reference, the tail can be seen in the brush in Fig. 2, the tail of a lower frequency comb line almost touches the higher frequency comb line directly above it). This asymmetric tail, also visible in other publications [16], is the main cause of crosstalk between modes, 4% of the peak intensity of each comb line appears at the location of the adjacent higher frequency line. In contrast, each mode only images 0.5% of its peak power to the adjacent comb line lower in frequency.

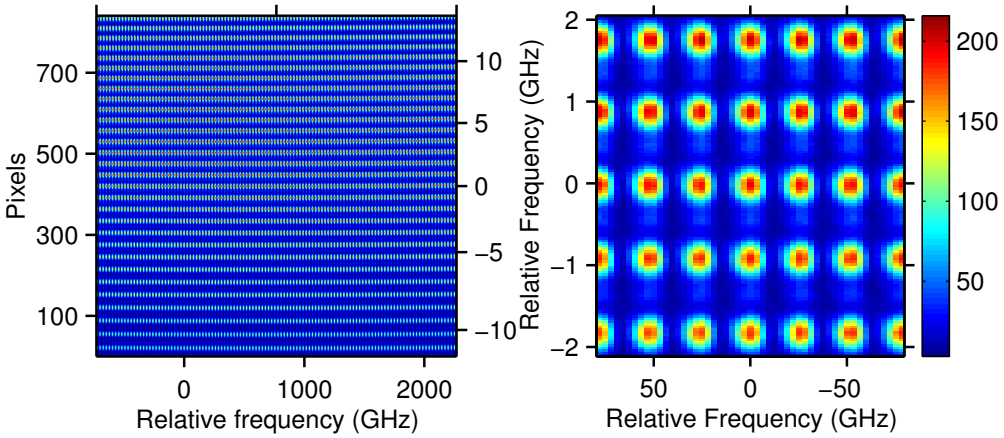

Fig. 2. Images showing a frequency brush of the resolved discrete frequencies of an 890 MHz pulse train. The image on the left shows the entire VIPA FSR and the image on the right shows a zoomed-in section of the spectrum. For the image on the left, the left vertical axis is labeled in pixels, whereas the right axis is labeled in frequency. For the image on the right, the difference between pixels and frequency is imperceptible.

Careful inspection of the entire VIPA FSR brush image in Fig. 2 reveals that modes near the bottom of the image are farther apart from one another in comparison to modes near the top of the image. Although these modes are equally spaced in frequency, the paraxial dispersion equation for the VIPA output angle has a nonlinear dependence on frequency [16]. To verify that the spacing between modes is as expected, the brush data is fit to this dispersion relation. This fit is done by first taking a vertical slice of the brush to measure the separation between modes dispersed by the VIPA and then converting the location of each mode to angle after the VIPA. The center frequency is set to 808 nm and each mode is separated by 890 MHz or 0.0019 nm (at 808 nm). Figure 3(b) shows a plot of the measured wavelength versus angle as well as a fit to the paraxial VIPA dispersion equation [15]

$$\Delta\lambda = -\lambda\left[\frac{\tan(\theta_{in})\cos(\theta_i)}{n\cos(\theta_{in})} + \frac{\theta_\lambda}{2n^2}\right] \tag{1}$$

where $\Delta\lambda$ is the difference in wavelength, λ is the center wavelength (808 nm), n is the index of refraction (1.44 for fused silica at 808 nm), θ_{in} is the angle of incidence (free parameter to be fit), and θ_i is the interior angle, set by θ_{in} and Snell's Law. The fit yields an angle of incidence of 1.0102° which is consistent with the measured angle of incidence of 1.01°.

#159985 - $15.00 USD Received 14 Dec 2011; revised 18 Jan 2012; accepted 20 Jan 2012; published 25 Jan 2012

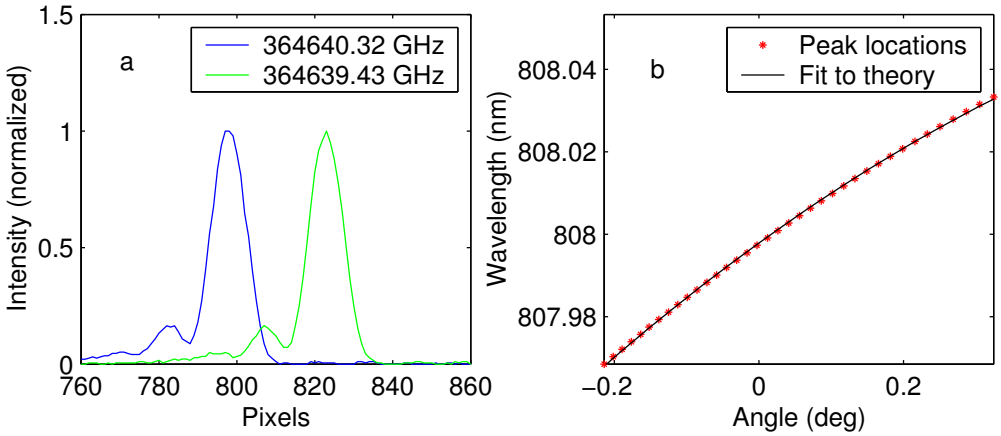

Fig. 3. (a) Two frequencies from the continuous wave laser separated by 890 MHz are used to calibrate the wavelength sensitivity and determine the resolution. They also show crosstalk between adjacent frequencies of the 890 MHz brush. (b) Measured wavelength vs. VIPA output angle (red circles) fit to paraxial VIPA dispersion law (black line).

In the current setup, the full bandwidth of the input pulse train cannot be used for pulse shaping due to the dispersion inside the fused silica VIPA, which results in a FSR that varies with frequency. To avoid this problem, an interference filter is used to filter the spectrum of the input pulse train to 10 nm FWHM.

Since many interesting and useful waveforms can be created using a repeating spectral mask, groups of equally spaced comb lines can be controlled together. This approach reduces the need to control all of the spectral channels individually, but still reveals important effects that are present even if they are individually controlled. By removing the grating and horizontal beam expander from the high resolution setup, a 1-D VIPA only pulse shaper [17] is created, Fig. 1(b). This configuration makes use of the repeating modes of the VIPA to control groups of comb lines together. However, a group does not correspond to adjacent comb lines, but rather all lines that are separated by one VIPA FSR. Thus our "group of lines" is quite different from prior work where this phrase has been used to indicate a group of adjacent comb lines. Since the VIPA still separates adjacent comb lines from one another, line-by-line pulse shaping is achieved with an effective mask that repeats every VIPA FSR. In this configuration, the VIPA separates adjacent modes from one another but overlaps modes separated by 25 GHz (VIPA FSR). This behavior means that every 28^{th} mode from the 890 MHz laser is imaged to the same location on the retro-reflecting mirror. It is essential that the FSR of the VIPA is exactly a multiple of the input laser repetition rate for the repeated modes of the VIPA to be imaged to the same location on the retro-reflecting mirror. Since FSR of the solid VIPA cannot be adjusted, the repetition rate of the laser is finely tuned to be $1/28^{th}$ of the FSR of the VIPA by adjusting the length of the laser cavity. The typical insertion loss of the pulse shaper is 15.2 dB and the lowest we observed was 13.3 dB.

3. Simulation

Under ideal conditions there is no difference between the 1-D VIPA based pulse shaper and one that separately resolves the individual comb lines from one another and uses a mask that repeats every VIPA FSR. In either case, dispersion inside the pulse shaper causes oscillations in the output spectrum with a period equal to the VIPA FSR. Although essentially dispersion-free operation can be achieved [17], our results suggest some dispersion remained in the current experiments. A simulation illustrates the spectral and temporal effects that dispersion has on the pulse shaper output.

The input to the simulation is an optical frequency comb with a Gaussian envelope. The blue comb in Fig. 4(c) shows a 50 GHz section of this input spectrum; since the width of the Gaussian envelope is very broad (1.2 THz) compared to the spacing between comb lines (890

#159985 - $15.00 USD Received 14 Dec 2011; revised 18 Jan 2012; accepted 20 Jan 2012; published 25 Jan 2012

MHz), the comb lines appear to have the same intensity. A figure that captures the full spectrum would show the overall Gaussian envelope, but comb lines would not be resolved. In the 1-D VIPA based pulse shaper, every 25 GHz section is treated the same. Thus only 50 GHz of the full spectrum is shown for each spectrum in Fig. 4.

Taking the Fourier transform of this simulated optical comb with constant phase, blue comb and green line illustrated in Fig. 4(c), yields the ideal time domain pulse train shown in Fig. 4(a). As expected, this ideal pulse train is identical to the input pulse train. To simulate how dispersion inside the pulse shaper affects the output pulse train, the input optical comb spectrum is multiplied by a phase mask that repeats every 28 spectral lines, or 25 GHz, as shown by the black curve in Fig. 4(c). The amplitude of the phase modulation is chosen to produce time-domain results that roughly match the experimental results shown below. The product is then Fourier transformed into the time domain (Fig. 4(b)). The effects of this phase mask that repeats every VIPA FSR is consistent with previous work on 1-D VIPA based pulse shapers where dispersion is present [17,18]. Due to the geometry of the pulse shaper, different groups of comb lines separated by the VIPA FSR take different paths. This results in a phase shift in the spectrum that repeats every VIPA FSR. The periodic nature of this modulation results in a temporal output that consists of bursts of pulses, as shown in Fig. 4(b). The pulses in each burst are separated by 40 ps, which is the inverse of the VIPA FSR. The peaks of the pulses map out an envelope that corresponds to what the output would be if the spectral width were restricted to one VIPA FSR.

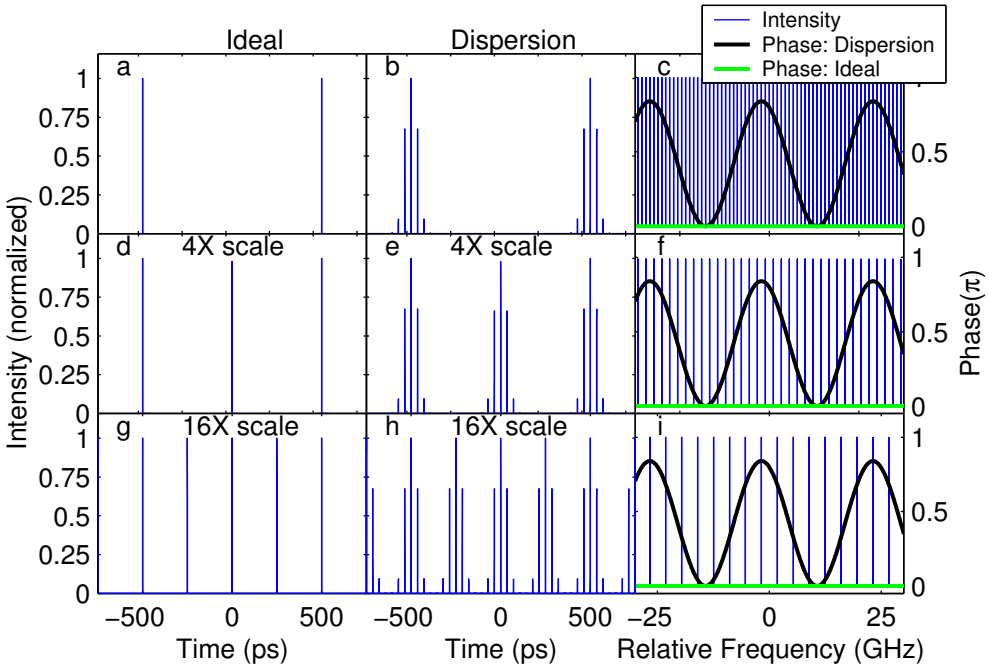

Fig. 4. Simulation of the temporal (first two columns) and spectral (last column) output of the 1-D VIPA based pulse shaper under ideal and non-ideal conditions for several masks. No mask (a-c), alternating comb mask (d-f), and a mask that blocks 3 out of every 4 comb lines (g-i) are shown. Time zero is chosen to be the time half-way between two pulses of the original pulse train. Under ideal conditions there is no phase modulation of the spectrum (flat phase illustrated in green) and when dispersion is present inside the pulse shaper there is periodic phase in the spectrum (illustrated in black).

Figures 4(d) and 4(f) show the ideal temporal and spectral effects of a mask that blocks every other comb line. As expected, the separation in frequency doubles, which halves the time between pulses in time. Likewise, an ideal mask that blocks 3 out of every 4 comb lines quadruples the separation in frequency and quarters the separation of pulses in time, Fig. 4(i)

#159985 - $15.00 USD Received 14 Dec 2011; revised 18 Jan 2012; accepted 20 Jan 2012; published 25 Jan 2012

and Fig. 4(g) respectively. The time domain response of the output when dispersion is present for the alternating comb mask, Fig. 4(e), is realized by taking the Fourier transform of the spectrum with periodic phase, blue comb and black curve shown in Fig. 4(f). Now each output pulse becomes a burst of narrow pulses under a Gaussian envelope similar to what was seen previously with dispersion in the no mask case. Since the mask doubles the comb spacing, we see half the time between pulse bursts. The time between the narrow pulses that comprise the pulse burst is still inverse the VIPA FSR, 40 ps. Finally, the Fourier transform of Fig. 4(i) with the periodic phase represented by the black curve is taken to produce the output pulse train for the mask that blocks 3 out of every 4 comb lines with dispersion, Fig. 4(h). Again we see the characteristic broadening of the pulses due to dispersion.

4. Experimental results

Figure 5 shows the intensity cross-correlations for the 1-D VIPA based pulse shaper described in Fig. 1(b). A beam splitter is used to send 50% of the input train of ~200 fs pulses (reference) to a delay stage which is then focused into a 5 mm thick β-BaB_2O_4 (BBO) crystal along with the output of the pulse shaper to generate a second harmonic signal only when two pulses are present. Due to the geometry of the cross-correlator, the length of the overlap region inside the large BBO crystal is only 0.466 mm, which corresponds to a phase matching bandwidth of 92 nm, more than enough to capture the full 10 nm FWHM spectrum of the pulse shaper output. By scanning the delay stage of the reference pulse, different time positions can be sampled. The cross-correlation data is then normalized by dividing the data by the peak intensity of the unmasked output.

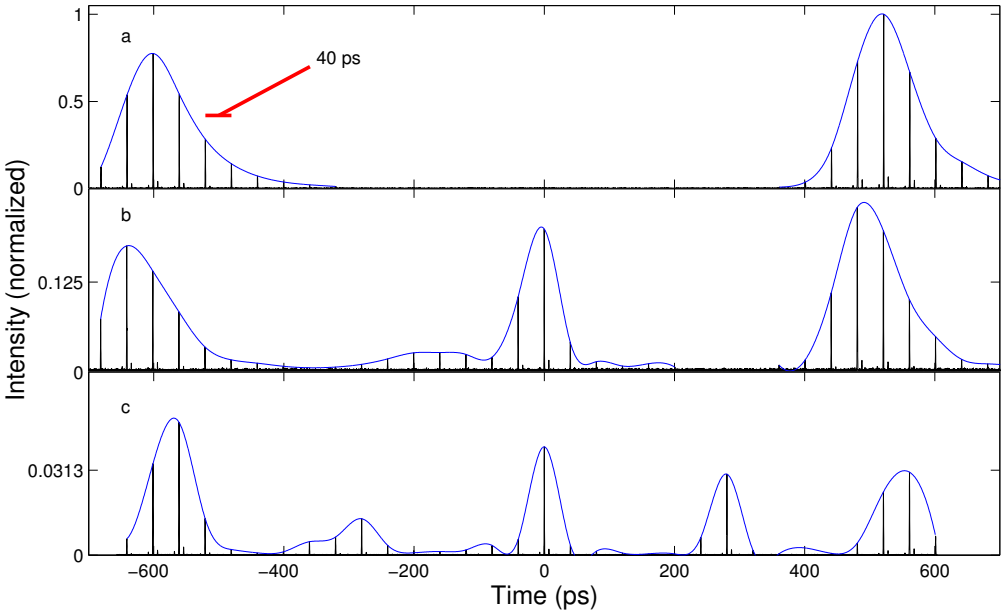

Fig. 5. Cross-correlation scans of pulse trains shaped by different line-by-line masks. Time zero is chosen to be the time half-way between two pulses of the unmasked pulse train. The first row (a) shows the output of the pulse shaper with no mask in place. An alternating comb line mask is used for the second row trace (b). The last row shows the output of the pulse shaper where 3 out of every 4 comb lines are blocked (c).

The output pulse train with no mask, Fig. 5(a), is not simply a reproduction of the input pulse train. As explained above by the simulation, the broadening of the pulse can be attributed to dispersion inside the pulse shaper. Similar to the simulation results, there is a burst of 600 fs pulses separated by 40 ps, the inverse of the VIPA FSR, under a Gaussian envelope. The smaller sidebands on each of these narrow pulses are the result of reflections in

#159985 - $15.00 USD Received 14 Dec 2011; revised 18 Jan 2012; accepted 20 Jan 2012; published 25 Jan 2012

the reference beam. The sub-pulses can be further suppressed by improved optimization of the dispersion, which in principle can be set to zero [18]. The suppression of the sub-pulses will then be limited by other variations over a VIPA FSR; for example variations in the amplitude due to clipping of higher diffraction orders or a mismatch between comb position and mask will also cause sub-pulses and thus set a limit on how well they can be suppressed.

Figure 5(b) illustrates the effect of a mask that blocks alternating comb lines in the plane of the mirror. The retro-reflecting mirror mask was created using photolithography to deposit an array of 150 μm wide by 3 cm long chrome rectangles separated by 150 μm onto an anti-reflection-coated piece of glass. This combination reflects every other group of frequencies within a single VIPA FSR. The peak intensity of the Gaussian envelope is close to the expected value of 1/4 the intensity of the no mask case. Figure 5(b) has a double pulse structure as well as discrete broadening of the pulse due to dispersion as was seen previously with the no mask case. In order to double the repetition rate, adjacent comb lines must be resolved, which makes this a good test case for line-by-line pulse shaping. The RF spectrum of the pulse shaper shows the fundamental of the repetition rate being suppressed by approximately 13 dB, which agrees with the approximate 4% cross-talk measured in section 2. The additional structure of the pulses can be attributed to the effect of imperfect mode matching of all 28 modes in the VIPA FSR to the mask. The dispersion law that defines how the VIPA separates adjacent comb lines from one another makes some adjacent comb lines closer together than others [19]. Since this difference in separation is minor, the static mask used in this experiment is a simple linear mask with a constant spatial period. However, spectral lines near the edges of every VIPA FSR are likely attenuated due to this mismatch between the mask and the spectral modes.

Other masks also demonstrate line-by-line pulse shaping. As demonstrated in Fig. 5(c), by blocking 3 out of every 4 comb lines, the expected quadruple pulse output is obtained. As expected, the peak intensity of the Gaussian envelope is approximately 1/16 of the intensity of the no mask case. Again, the effects of dispersion and imperfect mask matching are evident on the output pulse train. Although these effects are nonideal, they are not due to the fact that we use a one-dimensional spectral disperser and mask geometry; similar effects will be present even if a two-dimensional spectral and two-dimensional mask or modulator array are used to control a frequency brush (provided similar nonidealities in alignment remain).

5. Conclusion

A high resolution spectral disperser with resolution of 357 MHz has been demonstrated and used to resolve individual lines from an optical frequency comb. Line-by-line pulse shaping has been demonstrated for a mode-locked Ti:sapphire laser at 890 MHz repetition rate, the lowest rate for which line-by-line pulse shaping has yet been achieved. Such low repetition rate pulse shaping is an important step toward OAWG as it would potentially allow waveform updating to be achieved on a pulse-by-pulse basis with modulator arrays with relaxed speed requirements. Such experiments are needed in order to verify the compromise between switching speed and waveform fidelity predicted in [6].

Acknowledgments

Funding for this project was provided by NIST. AMW also acknowledges funding from the National Science Foundation under Grant ECCS-0601692.

#159985 - $15.00 USD Received 14 Dec 2011; revised 18 Jan 2012; accepted 20 Jan 2012; published 25 Jan 2012